Permeability-enhancing effects of three laurate-disaccharide monoesters across isolated rat intestinal mucosae

Fiona McCartney [a],[1], Diego R. Perinelli [b],[1], Mattia Tiboni [c], Robert Cavanagh [d], Simone Lucarini [c], Giovanni Filippo Palmieri [b], Luca Casettari [c],[*], David J. Brayden [a],[*]

[a] UCD School of Veterinary Medicine and UCD Conway Institute, University College Dublin, Belfield, Dublin 4, Ireland
[b] School of Pharmacy, University of Camerino, Via Gentile III da Varano, 62032 Camerino, MC, Italy
[c] Department of Biomolecular Sciences, University of Urbino Carlo Bo, Piazza del Rinascimento, 6, 61029 Urbino, PU, Italy
[d] Division of Molecular Therapeutics and Formulation, School of Pharmacy, University of Nottingham, Nottingham NG7 2RD, United Kingdom

ARTICLE INFO

ABSTRACT

Laurate (C_{12})-sucrose esters are established intestinal epithelial permeation enhancers (PEs) with potential for use in oral delivery. Most studies have examined blends of ester rather than specific monoesters, with little variation on the sugar moiety. To investigate the influence of varying the sugar moiety on monoester performance, we compared three monoesters: C_{12}-sucrose, C_{12}-lactose, and C_{12}-trehalose. The assays were: critical micellar concentration (CMC) in Krebs-Henseleit buffer, MTS and lactate dehydrogenase assays in Caco-2 cells, transepithelial electrical resistance (TEER) and apparent permeability coefficient (P_{app}) of [^{14}C] mannitol across isolated rat intestinal mucosae, and tissue histology. For CMC, the rank order was C_{12}-trehalose (0.21 mM) < C_{12}-sucrose (0.34 mM) < C_{12}-lactose (0.43 mM). Exposure to Caco-2 cells for 120 min produced TC_{50} values in the MTS assay from 0.1 to 0.4 mM. Each ester produced a concentration-dependent decrease in TEER across rat mucosae with 80% reduction seen with 8 mM in 5 min, but C_{12}-trehalose was less potent. C_{12}-sucrose and C_{12}-lactose increased the P_{app} of [^{14}C] mannitol across mucosae with similar potency and efficacy, whereas C_{12}-trehalose was not as potent or efficacious, even though it still increased flux. In the presence of the three esters, gross intestinal histology was unaffected except at 8 mM for C_{12}-sucrose and C_{12}-lactose. In conclusion, the three esters enhanced permeability likely via tight junction modulation in rat intestinal tissue. C_{12}-trehalose was not quite as efficacious, but neither did it damage tissue to the same extent. All three can be considered as potential PEs to be included in oral formulations.

1. Introduction

Delivery of poorly permeable macromolecules and Biopharmaceutical Class III small molecules across the intestine remain one of the great challenges for pharmaceutical scientists. Three main strategies are currently being pursued: formulation of molecules with intestinal permeation enhancers (PEs), entrapment in nanoparticles, and the use of intestinal microneedle and patch devices (Brayden et al., 2020). Of these, the most clinically-advanced oral formulations for peptides are those that incorporate the use of PEs. Yet, despite the recent Food and Drug Administration (FDA) approvals of oral versions of semaglutide and octreotide, the oral bioavailability of these formulations using PEs is estimated at ~1% (Tuvia et al., 2012; Buckley et al., 2018). Recently, a high throughput screen of PEs using explants of porcine jejunum concluded that systematic assessment of PEs has barely begun and will yield more efficacious and safe candidates for oral formulation with macromolecules (Von Erlach et al., 2020). With this in mind, we sought to investigate chemical variations of disaccharide conjugate monoesters of the established salt of the medium-chain fatty acid PE, laurate (C_{12}) (Dittmann et al., 2014).

We recently established that the food-grade surfactant, the sucrose laurate ester, D1216, could increase fluxes of marker molecules in Caco-2 monolayers and isolated rat intestinal tissue mounted in Ussing chambers (McCartney et al., 2019a). Moreover, in rat intestinal jejunal and colonic instillations, it delivered insulin with relative bioavailability values of 2.4% and 8.9% respectively, similar to values obtained with

the established PE, sodium caprate (C_{10}). The D1216 form of sucrose laurate is a blend of mono-, di- and tri-esters, so the question arises as to whether a mono-ester format, i.e. a selective 6-O-sugar fatty acid monoester of sucrose laurate, would be as efficacious. There is particular interest in pursuing sugar mono-esters as PEs for oral delivery of macromolecules as these amphiphiles are biodegradable and non-toxic with a history of use in humans and can be made with green chemistry (Lucarini et al., 2016).

In parallel, attempts have been made to vary the sugar moiety from sucrose and the carbon chain length on resulting monoesters. Lucarini et al. explored the capacity of C_{10}, C_{12}, C_{14}, and C_{16} monoesters of lactose to reduce transepithelial electrical resistance (TEER) across Caco-2 monolayers and attempted to relate cytotoxicity to critical micellar concentration (CMC) [8]. Lactose esters with long-chain lengths had lower CMCs, reflecting an increased hydrophobicity and high capacity to insert into plasma membranes, which were accompanied by lower TC_{50} values in cytotoxicity assays. Of the four esters, only C_{12}-lactose reduced TEER across Caco-2 monolayers. The two main conclusions of the study were that non-ionic surfactants are more likely to cause toxicity if their CMC is low and that the C_{12} chain length could be a useful template to build ester variations around in respect of finding new PEs.

In the current study, we compared three sugar mono-ester variants of C_{12} head-to-head across selected criteria. Sucrose laurate was supplied from a vendor in a mono-ester format and designated as C_{12}-sucrose, as distinct from the D1216 blend used previously (McCartney et al., 2019a). Lactose monolaurate (C_{12}-lactose) was the second variation selected as it had shown initial promise by reducing TEER across Caco-2 monolayers (Lucarini et al., 2018). The third was a newly synthesised construct, trehalose monolaurate (C_{12}-trehalose), which was attractive given the current use of trehalose as a cryo-protective non-toxic excipient in lyophilised formulations (Izutsu, 2018). C_{12}-sucrose has rarely been assessed for PE potential in a monoester format, one example being a screening study of surfactant-type PEs in isolated rat colonic mucosae (Maher et al., 2018) where it was in the mid-range of PEs regarding capacity to stimulate flux of [^{14}C]-mannitol. C_{12}-lactose has only been tested for PE potential indirectly using Caco-2 monolayers, while to our knowledge C_{12}-trehalose has not yet been tested as a PE. The assays used to compare the three esters were: the MTS and lactate dehydrogenases assays in Caco-2 cells, the Laurdan assay in Caco-2 cells, the CMC values in Kreb's Henseleit (KH) buffer, TEER and the apparent permeability coefficient (P_{app}) values of [^{14}C] mannitol across rat intestinal tissue mucosae, and the histology of mucosae. The three agents had similarly low CMC values and TC_{50} values in the cytotoxicity assays with no obvious patterns. The main finding was that all three esters increased permeability across the isolated intestinal mucosae without damaging tissue at selected concentrations.

2. Materials and methods

2.1. Synthesis of lactose monolaurate and trehalose monolaurate

C_{12}-sucrose (MW 525 Da) was purchased from Sigma-Aldrich (Ireland). C_{12}-lactose (MW 525 Da) and C_{12}-trehalose (MW 525 Da) were synthesised using our previous methods for both substances (Lucarini et al., 2018; Elmowafy et al., 2020). They were obtained by chemical synthesis using an enzymatic approach, which used either lactose monohydrate or trehalose monohydrate, as well as lauric acid as starting materials. For the synthesis of C_{12}-lactose, 2.4 U Lipozyme® (immobilized from *Mucor miehei*) (Sigma-Aldrich) with a specific activity of >30 U/g (0.078 g) was used as a catalyst. It was added to a solution of lauric acid (0.79 mmol) and lactose tetra acetate (0.79 mmol) in water-saturated toluene. The mixture was stirred at 75 °C for 12 h, cooled and diluted with acetone before the removal of the enzyme by filtration. The filtrate was concentrated and purified by column chromatography giving a pale-yellow oil. The oil was then dissolved in

tetrafluoroboric acid diethyl ether complex/water/acetonitrile (2.1 mL, 1: 5: 500) and stirred at 30 °C for 3 h. The white solid precipitated was filtered, washed with acetonitrile, and dried. Finally, purification by recrystallization from methanol gave the final product as white solid.

For the synthesis of C_{12}-trehalose, triethylamine (130.9 mmol) was added to a stirred suspension of trehalose (3.27 mmol) in dichloromethane (DCM) (15 mL). The reaction mixture was cooled to 0 °C, and trimethylsilyl chloride (39.26 mmol) was added. The solution was stirred at room temperature (RT) for 12 h, and then an additional 13.08 mol of trimethylsilyl chloride were added at 0 °C. The reaction was left to stir for an additional 4 h at RT and then the solvents were evaporated using a rotor to extract the crude product with petroleum ether. The organic layers were concentrated by vacuum to obtain a cream-yellow intermediate that was then solubilized in a cooled solution of methanol and DCM (19 mL, 3:1) at 0 °C. Potassium carbonate (0.40 mmol) was added and the reaction was stirred for 15 min at 0 °C and then at RT for 1 h. The reaction was quenched by the addition of acetic acid (0.7 mL). The solvents were removed by vacuum and the product was purified by column chromatography before placement in a flame-dried Schlenk flask with 4-DMAP (1.30 mmol) and lauric acid (1.30 mmol) in 5 mL of anhydrous DCM. A solution of 1,3-DCC (1.20 mmol) in anhydrous DCM (3 mL) was added dropwise. The mixture was left to react overnight at RT, under a nitrogen atmosphere. The resulting precipitate was removed by filtration under reduced pressure, washed with dichloromethane and purified by flash column chromatography. Finally, to obtain the ester, the intermediate was added to 0.5 mL of a 3:1 DCM / methanol solution with 10% w/w of Dowex-H$^+$. After 30 min stirring at RT, the mixture was filtered and concentrated by vacuum, and the resulting residue was crystallized to obtain C_{12}-trehalose. The purity of the synthesised C_{12}-lactose and C_{12}-trehalose was estimated from ^{1}H NMR to be ≥95%, while Sigma's data sheet specification for C_{12}-sucrose states a value of ≥97%. The structures of the three esters are shown (Fig. 1).

2.2. Surface tension measurements and critical micellar concentrations

The surface tension of the monolaurate esters in KH buffer was measured using a platinum cylindrical rod probe with a wetted length of 1.6 mm (K100-Krüss force tensiometer, Hamburg, Germany). Approximately 1 mL of each surfactant solution was placed on a Teflon plate and the surface of the liquid was aspirated to remove remaining impurities. The rod probe was then immersed 2 mm into the liquid and then retracted. Data are expressed as the mean of three repeated measurements performed at RT. The critical micelle concentration (CMC) and the surface tension at the CMC (γCMC) were calculated by a segmental linear regression approach (Prism-5® software, San Diego, CA, USA, article #1101).

2.3. MTS and LDH cytotoxicity studies on Caco-2 cells

Caco-2 human colonic cancer cells were obtained from the American Type Culture Collection (ATCC; Manassas, Virginia) and were used at passages 30–40. Cells were cultured in Dulbecco's modified eagle medium (DMEM; Sigma-Aldrich) supplemented with 10% (v/v) foetal bovine serum (FBS; Sigma-Aldrich), 0.1 mg/mL of streptomycin, 100 units/mL of penicillin, 0.25 μg/mL of amphotericin (Sigma-Aldrich), and 2 mM L-glutamine (Sigma-Aldrich) at 37 °C with 5% CO_2. The MTS ((3-(4,5-dimethylthiazol-2-yl)-5-(3-carboxymethoxyphenyl)-2-(4-sulfophenyl)-2H-tetrazolium)) cell proliferation assay (CellTiter 96 Aqueous Cell Proliferation Assay, Promega) and the lactate dehydrogenase (LDH) release assay (Sigma-Aldrich, TOX7 kit) were used. Caco-2 cells were seeded at a density of 1×10^4 cells per well in 96-well plates (Corning) for 48 h before assay. Cells were exposed to C_{12}-sucrose, C_{12}-lactose and C_{12}-trehalose in 100 μl DMEM at concentrations of 0.05, 0.075, 0.1, 0.2, 0.5, 0.75 and 1 mM for 24 h. DMEM was used as the vehicle control and 1% (v/v) Triton® X-100 (TX) in DMEM was a positive control. Following the 24 h exposure period, 50 μl of supernatant was collected per well for
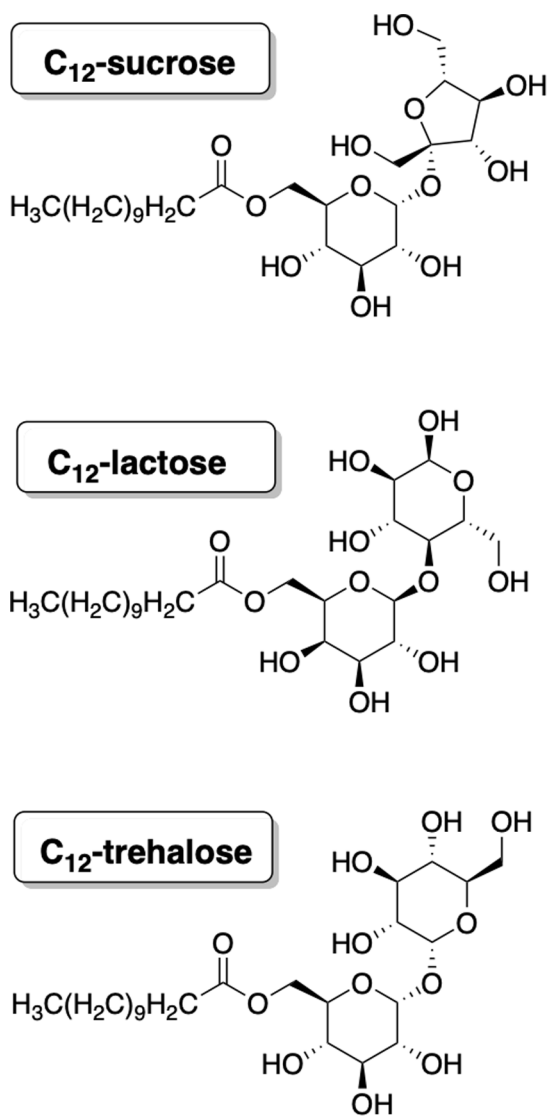
Fig. 1. Chemical structure of the monoester sugar-based surfactants.

analysis of LDH content. Cells were then washed with warm PBS and 120 μl MTS solution (17% v/v applied in DMEM) for 120 min after which the absorbance was measured at 492 nm using a UVM 340 plate reader (ASYS Hitech GmbH, Austria). Activity in the MTS assay was calculated by setting values from the vehicle control as 100% and positive control values as 0% metabolic activity. Assessment of LDH release was performed according to the manufacturer's instructions and involved adding 100 μl LDH reagent to collected supernatant samples and incubation at RT with shielding from light for 25 min. Absorbance was then measured at 492 nm. Relative LDH release was calculated with the negative control absorbance at 492 nm taken as 0%, and the positive control as 100%.

2.4. Laurdan fluidization assay in Caco-2 cells

To assess the effect of sugar esters on Caco-2 plasma membrane fluidity, the Laurdan probe (Thermo Fisher Scientific) was used (Sanchez et al., 2012). Caco-2 cells were cultured as above for 48 h before assay. Culture media was removed and cells incubated with 10 μM Laurdan solution applied in Hank's Balanced Salt Solution (HBSS, Sigma-Aldrich) for 30 min at 37 °C. Laurdan solutions were then removed, cells washed with HBSS twice and 100 μl HBSS buffer returned to each well. Fluorescence was excited at 380 nm and the emission

intensity was read at 440 nm and 490 nm (I440 and I490, respectively) every 1 min for 5 min to establish baseline levels of generalized polarization (GP). Buffer was then removed from wells, by gentle pipetting. 100 μl of C_{12}-sucrose, C_{12}-lactose, and C_{12}-trehalose was applied in HBSS at concentrations of 0.2, 0.5 and 1.0 mM. Fluorescent intensities were then obtained every min over 20 min. GP values were calculated using the equation, GP = (I440 - I490)/(I440 + I490), (Parasassi et al, 1991).

2.5. Ex vivo studies on isolated rat colonic mucosae: dissection and electrophysiology

Colonic- rather than small intestinal mucosae were used because the former is easier to dissect free of underlying smooth muscle, is more robust against mounting in Ussing chambers, and can better discriminate effects of PEs (e.g. Stuettgen and Brayden, 2020). All studies were carried out under UCD Animal Research Ethics Committee Protocol Number "14-28-Brayden." Adult male Wistar-CRL rats were obtained from Charles River Laboratories, UK, and were housed in a pathogen-free environment with controlled conditions of humidity and temperature under a 12:12 h light/dark cycle with access to laboratory chow and filtered water ad *libitum*. Rats weighing 250–400 g were euthanized by stunning and cervical dislocation. A midline laparotomy was performed, and the colon was excised and placed directly in KH buffer in de-ionised water at a pH of 7.4 and with bubbling with carbogen. After stripping the circular and longitudinal muscle layers with a size #5 watchmaker forceps, rat colonic mucosae was mounted in Ussing chambers with a circular window area of $0.63\ cm^2$, bathed bilaterally with 5 mL of KH buffer, and continuously bubbled with a mixture of O_2 and CO_2 (95%/ 5%) (Twarog et al., 2021). After 45 min pre-incubation of tissue in chambers KH buffer was replaced with sugar monoester solution dissolved in KH in the donor-side compartment of the chamber apparatus.

The potential difference (PD, mV) was recorded in an open circuit configuration for a 15-min equilibration period after which the tissue was voltage-clamped using an Epithelial Voltage Clamp (EVC 4000; WPI, Hitchin, UK). Short-circuit current (Isc, $\mu A\ cm^{-2}$) and PD were monitored by switching from clamp to open circuit, respectively, for 3 s every 30 s using a Pro 4® timer (AD Instruments, Oxford, UK). The analogue signals were digitized using a Powerlab® data acquisition module, and the data were analyzed using LabChart® software (AD Instruments). Transepithelial electrical resistance (TEER, ohm. cm^2) was calculated using Ohm's Law. At the end of each flux in the presence of esters, the capacity of colonic mucosae to generate a transient inward Isc in response to basolateral addition of the non-specific acetylcholine receptor agonist, carbachol (0.1, 1.0, and 10 μM). This assay was used to assess tissue functionality (Maher et al., 2009).

2.6. [^{14}C]-mannitol permeability studies

After tissue equilibration for 30 min, [^{14}C] mannitol was added (specific activity: 0.1 $\mu Ci\ mL^{-1}$) to the apical side of the Ussing apparatus. Samples at 0, 20, 40, 60, 80, 100, 120 min were taken from the basolateral side of the chamber (200 μl) and replenished with KH buffer. Samples were mixed with a scintillation fluid (Ecoscint A; National Diagnostics, USA) and the disintegrations per minute (dpm) were determined using a Packard Tricarb 2900 TR scintillation counter. The apparent permeability coefficient (P_{app}) of mannitol across colonic mucosae was calculated according to the following equation:

$$P_{app} = dQ/dt(1/A*C_0),$$

where dQ/dt is the transport rate across epithelium (dpm. s^{-1}), A is the exposed area of the tissue ($0.63\ cm^2$), and C_0 is the initial concentration added to the donor compartment (dpm. mL^{-1}).

2.7. Histology of exposed colonic mucosae

Following the exposure of rat intestinal tissue mucosal sheets to esters in Ussing chambers, tissues were immersed in 10% (v/v) buffered formalin for at least 48 h and subsequently embedded in paraffin wax. Tissue sections (5 μm) were cut on a microtome (Leitz 1512; GMI, USA), mounted on adhesive-coated slides, and stained with haematoxylin and eosin (H & E). The slides were visualised under a light microscope (NanoZoomer 2.0-HT light microscopy (Hamamatsu)) and images were taken with a high-resolution camera (Micropublisher 3.3 RTV; Q Imaging, Canada) and Image-Pro Plus version 6.3 (Media Cybernetics Inc., USA) acquisition software.

2.8. Statistical analysis

The analysis was carried out using Prism-5® software (GraphPad, USA). ANOVA one-way with Dunnett's *post hoc* multiple comparison tests were used to assess changes in GP in the Laurdan assay over time. A two-way ANOVA with Dunnett's *post-hoc* test was used to compare data from groups for TEER values and a two-way ANOVA with Dunnett's *post-hoc* test was used to compare groups in [^{14}C]-mannitol P_{app} experiments. Results are given as mean ± SEM (or SD in some studies) from a minimum of three independent experiments. A significant difference was considered as present if P < 0.05.

3. Results and discussion

3.1. Surface tension analysis and CMC determination of the esters

The three monoesters had similar surface adsorption properties, as revealed by tensiometry measurements (Fig. 2). The CMC values for all three agents ranged between 0.20 mM and 0.45 mM in KH solution, while the surface tension at the CMC (γCMC) was between 35 and 38 mN/m for the three esters. Surface properties typically relate to the mono-esterification on C_6 of the sugar moiety and the length of the carbon chain, common features for these amphiphiles (Gaudin et al., 2018; Baghban et al., 2018). While the type of disaccharide forming the polar head is usually less relevant, the CMC values increased in the order: C_{12}-trehalose (CMC: 0.21 mM) < C_{12}-sucrose (CMC: 0.34 mM) < C_{12}-lactose (CMC: 0.43 mM). A trend was also observed for the other adsorption parameters such as the surface excess concentration (Γ_{max}) and the minimum area per molecule (A_{min}). Specifically, the A_{min} slightly decreased for the C_{12} monoesters in the order: C_{12}-trehalose > C_{12}-lactose > C_{12}-sucrose (Table 1). As previously observed for other
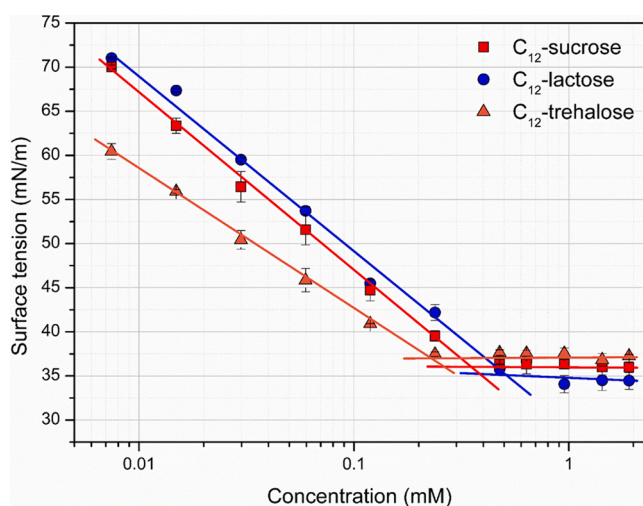

Fig. 2. Surface tension vs concentration for the three mono-ester sugars in KH buffer.

Table 1
Tensiometric measurements for the monoester sugars.

Entry	CMC (mM)	γCMC (mN/m)	Γ_{max} *10^{-6} (mol/m²)	A_{min} (Å²)
C_{12}-sucrose	0.34 ± 0.02	36.9 ± 0.4	4.60 ± 0.32	36.02 ± 1.24
C_{12}-lactose	0.43 ± 0.02	34.9 ± 0.3	4.36 ± 0.14	38.14 ± 0.89
C_{12}-trehalose	0.21 ± 0.01	37.5 ± 0.3	4.21 ± 0.18	39.44 ± 0.74

CMC, critical micellar concentration; surface tension at CMC (γCMC); surface excess concentration (Γ_{max}); minimum area per molecule (A_{min}).

sugar surfactants, the use of a physiological buffer such as KH did not alter the surface and aggregation properties of 6′-O-monolaurate sugar-based surfactants compared to values obtained in water (Garofalakis et al., 2000). Previously, a CMC value of 0.55 mM for C_{12}-lactose was obtained in water (Lucarini et al., 2018), so there appears only a slight difference when measuring the CMC in KH for these esters.

3.2. Cytotoxicity of the esters on Caco-2 cells: MTS assay and LDH release

Cytotoxic effects of the three mono-esters were evaluated in Caco-2 intestinal cells using the MTS assay and the LDH release assay for 24 h exposures (Fig. 3). The TC_{50} values for the MTS assay were 0.28 mM (95% CI: 0.25–0.31 mM), 0.36 mM (95% CI: 0.32–0.41 mM) and 0.48 mM (95% CI: 0.47–0.49 mM) for C_{12}-sucrose, C_{12}-lactose, and C_{12}-trehalose, respectively (Fig. 3A). The LDH release assay provided TC_{50} values of 0.27 mM (95% CI: 0.23–0.31 mM), 0.34 mM (95% CI: 0.30–0.41 mM) and 0.41 mM (95% CI: 0.31–0.51 mM) for C_{12}-sucrose, C_{12}-lactose, and C_{12}-trehalose, respectively (Fig. 3B). Taken together, both assays indicate a rank order in terms of cytotoxicity as C_{12}-sucrose > C_{12}-lactose > C_{12}-trehalose, but with all values in the 0.2–0.5 mM range over the long exposure period. There were no statistical differences between the TC_{50} values within or between the two assays. The three agents were much less cytotoxic than Triton®-X-100.

3.3. Effect of the esters on Caco-2 plasma membrane fluidity: the Laurdan assay

Laurdan GP analysis demonstrated that Caco-2 cells had a baseline GP of 0.21 ± 0.02, in agreement with literature results (Cavanagh et al., 2019; Verstraeten et al., 2013). Upon addition of the three esters to Caco-2 cells, a concentration-dependent decline in GP values was observed at 1 min, indicating membrane fluidisation (Fig. 4). Following this initial reduction, GP values remained steady between 1 and 20 min at all tested concentrations, indicating that no further membrane fluidisation occurred within this time frame. Exposure to 0.2 mM C_{12}-sucrose, C_{12}-lactose and C_{12}-trehalose, elicited very small decreases in GP values at 1 min to 0.200 ± 0.007 (mean Δ_{GP}: 0.016; P > 0.05), 0.201 ± 0.006 (mean Δ_{GP}: 0.014; P > 0.05) and 0.206 ± 0.013 (mean Δ_{GP}: 0.010; P > 0.05), respectively, not statistically different from controls (one-way ANOVA followed by Dunnett's multiple comparison test). At 0.5 mM, however, within 1 min of exposure, each ester reduced GP significantly compared to control values with C_{12}-sucrose decreasing GP to 0.164 ± 0.015 (mean Δ_{GP}: 0.049; P < 0.0001), C_{12}-lactose to 0.174 ± 0.006 (mean Δ_{GP}: 0.039; P < 0.001) and C_{12}-trehalose to 0.195 ± 0.011 (mean Δ_{GP}: 0.019; P < 0.05). The decrease in GP elicited by 0.5 mM C_{12}-sucrose was noted to be statistically greater (P < 0.01) than that induced by 0.5 mM C_{12}-trehalose. Application of the monoesters at concentrations of 1.0 mM induced the largest declines in GP. The resulting GP values following 1 min of exposure to 1 mM were 0.140 ± 0.009 (mean Δ_{GP}: 0.076; P < 0.0001), 0.152 ± 0.010 (mean Δ_{GP}: 0.064; P < 0.0001) and 0.174 ± 0.011 (mean Δ_{GP}: 0.042; P < 0.0001), for C_{12}-sucrose, C_{12}-lactose and C_{12}-trehalose, respectively. At 1.0 mM, the change in GP
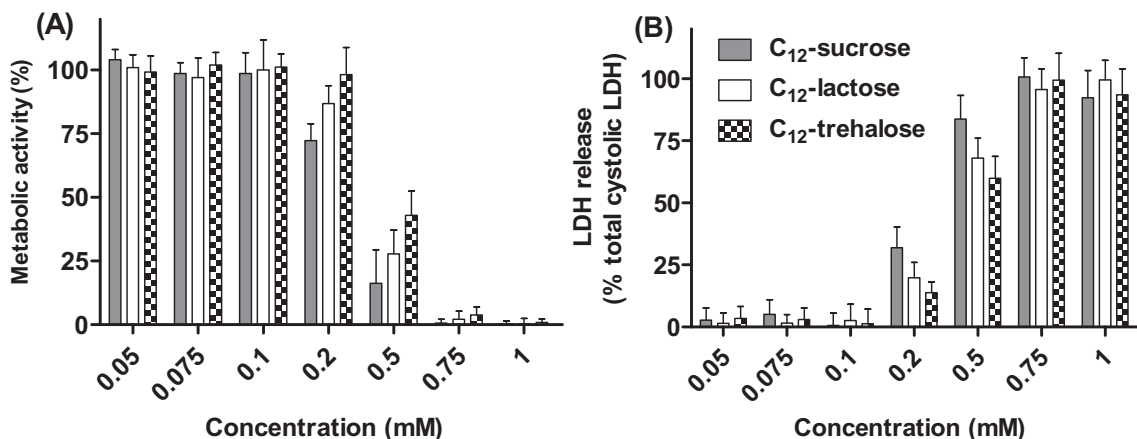
Fig. 3. Cytotoxicity of monoesters on Caco-2 cells as indicated by (A) MTS and (B) LDH release assays. Monoesters were incubated on cells for 24 h. Data are presented as mean ± S.D (n = 3).
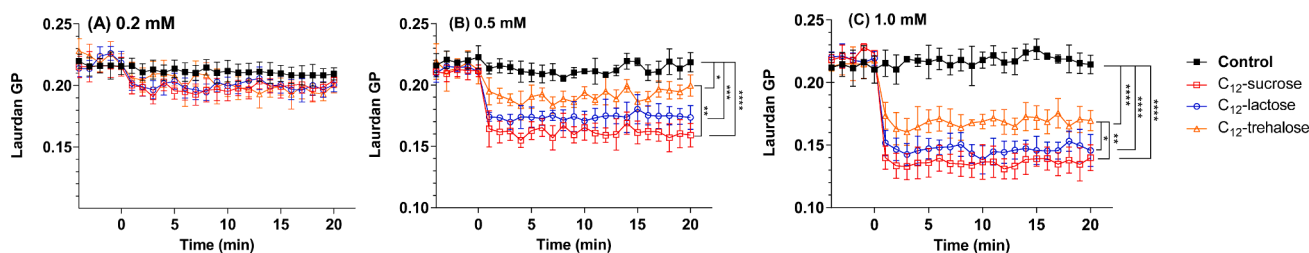

Fig. 4. Effect of monoesters on Caco-2 plasma membrane fluidity as measured by Laurdan GP. Monoesters were applied to cells in HBSS buffer for 20 min, with GP measured every min. (A). 0.2 mM, (B) 0.5 mM, (C) 1 mM. Data are mean ± S.D (n = 3). Statistical significance was determined between treatments at first min of exposure. *P < 0.05; **P < 0.01; ***P < 0.001; ****P < 0.0001.

induced by C_{12}-trehalose was significantly less than that of C_{12}-sucrose (P < 0.01) and C_{12}-lactose (P < 0.05). No statistical differences between C_{12}-sucrose and C_{12}-lactose were found at any of the tested concentrations.

From the Laurdan data, it can be ascertained that the three esters induced a rapid increase in Caco-2 apical membrane fluidity, which was consistent with surfactant insertion into the membrane structure. Significant fluidisation was observed when 0.5 mM concentrations above the CMCs of the three esters were applied, indicating an association with micelles. These likely act as reservoirs to supply surfactant monomers to participate in further membrane interactions (Shubber et al., 2015; Preté et al., 2011; Lichtenberg et al., 2013). On the contrary, C_{12}-trehalose (CMC: 0.21 mM), surprisingly did not induce fluidisation at 0.2 mM, suggesting that C_{12}-trehalose is less capable of interacting with the phospholipid bilayer of the plasma membrane than the other esters

despite its lower CMC value. The Laurdan data demonstrates that the monoester potency in inducing plasma membrane fluidisation can be ranked as C_{12}-sucrose ≥ C_{12}-lactose > C_{12}-trehalose. In McCartney et al. (2019a) the sucrose laurate blend (D1216) decreased plasma membrane potential in Caco-2 cells at 1 mM over 60 min and at 0.5 mM at 24 h. Together with the LDH data, these patterns are consistent with the membrane effects of ester surfactants.

3.4. Ex vivo rat intestinal mucosae TEER changes in response to the esters

For all three esters, apical-side additions caused concentration-dependent reductions in TEER across isolated rat colonic mucosae (Fig. 5). C_{12}-sucrose and C_{12}-lactose induced similar patterns, more dramatic than for C_{12}-trehalose. For 0.5 mM concentrations of each, a slight decrease in TEER was recorded over 40 min, no different from
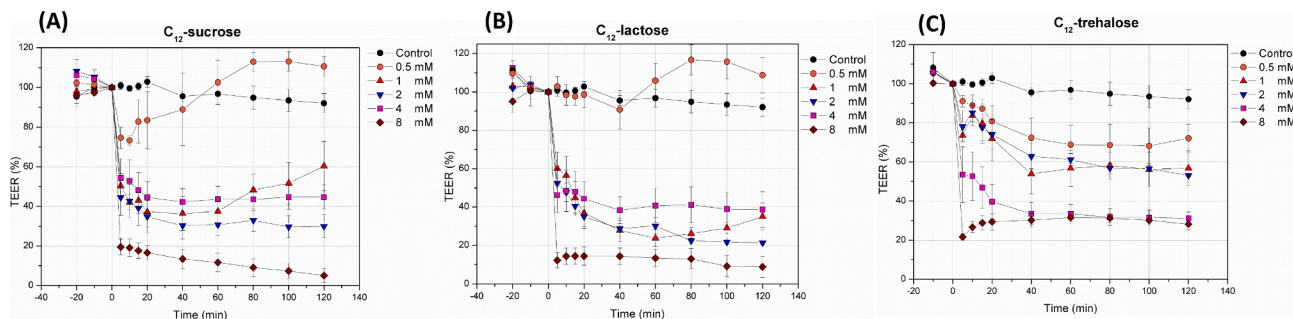

Fig. 5. Effects on TEER across rat colonic mucosae after exposure to sugar esters. (A) C_{12}-sucrose, (B) C_{12}-lactose, (C) C_{12}-trehalose. Data are mean ± SEM (n = 4–8). Significant differences between treatments and controls were detected from 5 min to 120 min after addition of C_{12}-sucrose and C_{12}-lactose at 1 mM, 2 mM, 4 mM, 8 mM, and for C_{12}-trehalose at 4 mM and 8 mM (***P < 0.001 in each case). Statistical differences were also seen for C_{12}-trehalose from 60 min to 120 min at 0.5 mM (*P < 0.05), and from 20 min to 120 min for at 1 mM and 2 mM (**P < 0.01).

control (Fig. 5 A, B). For concentrations of 1–4 mM, a reduction to 30–45% of control values was observed. TEER values decreased immediately after ester addition and reached a plateau after 40 min. A still further decrease in TEER was achieved with 8 mM concentrations, where values decreased to ~20% of control within 5 min.

In general, C_{12}-trehalose had a less potent effect on TEER reduction compared to the other two esters, despite causing a statistically decrease in TEER to 70% of control at 0.5 mM (P < 0.05, Fig. 5C). The difference can be partially ascribed to CMC differences. Surfactant aggregation and the CMC can impact TEER at a concentration of 0.5 mM. At this concentration, surfactant adsorption to the mucosa in the form of micelles and mixed micelles is thermodynamically favoured for the trehalose monoester (CMC: 0.21 mM), slightly more than the sucrose and lactose monoesters, which have higher CMC values of 0.34 and 0.43 mM respectively and will therefore be present in higher free concentrations. The more dramatic effects of C_{12}-sucrose - and C_{12}-lactose in reducing TEER compared to C_{12}-trehalose can be ascribed to structural characteristics of the sugar moieties including the conformation and stereochemistry differences of these disaccharides. All three agents likely interact with tight junction proteins to cause openings (Kiss et al., 2014; Mine and Zhang, 2003).

3.5. Effects of the esters on the P_{app} of mannitol across rat colonic mucosae

The basal P_{app} for [^{14}C] mannitol across rat colonic mucosae was 2.3–2.6 × 10^{-6} cm/s, within the published range (McCartney et al., 2019b; Twarog et al., 2021). Increasing concentrations of the sugar monoesters induced a higher P_{app} for the [^{14}C] mannitol marker (Fig. 6), a paracellular flux increase associated with tight junction openings both in this model (Bzik and Brayden, 2016) and also in Caco-2 monolayers (Antonescu et al., 2019). A statistical increase in the [^{14}C] mannitol P_{app} was observed for C_{12}-sucrose at 8 mM (P < 0.0001), for C_{12}-lactose at concentrations > 1 mM (P < 0.01), and for C_{12}-trehalose at 4 mM (P < 0.01) and 8 mM (P < 0.001). Overall, there were comparable increases in the P_{app} for both C_{12}-lactose and C_{12}-sucrose at equivalent concentrations. At concentrations in the low mM range, there was a mean 3.1–3.6-fold increase in the P_{app} for C_{12}-sucrose and a mean 2.8–3.7-fold increase for C_{12}-lactose, but only an increasing trend for C_{12}-trehalose. At 8 mM, the average increase was 5.4-fold for C_{12}-lactose, 8.8-fold for C_{12}-sucrose, and 3.2 fold for C_{12}-trehalose. The highest P_{app} was detected for C_{12}-sucrose at 8 mM and it corresponded with the lowest TEER value recorded (close to zero after 120 min). The lower effect of C_{12}-trehalose on the P_{app} (albeit statistically significant at higher concentrations) was consistent with its lower effects on TEER than the other two esters. Overall, the increased P_{app} values of [^{14}C] mannitol across rat colonic mucosae induced by C_{12}-sucrose and C_{12}-lactose inversely correlated with their capacity to reduce TEER.

3.6. Carbachol-induced I_{sc} in isolated rat colonic mucosae

The maintenance of functional capacity of colonic mucosae following ester exposure was assessed by measuring the inward I_{sc} induced by carbachol. Some minor differences amongst the esters can be noticed only on the I_{sc} response to 10 μM carbachol, but not at the two lower concentrations of the agent (0.1 and 1.0 μM) where I_{sc} responses were fully maintained at all concentrations of each ester. The ΔI_{sc} values observed for 10 μM carbachol were 60–80 μA cm^{-2} alone and in the presence of all tested C_{12}-trehalose concentrations, and also at concentrations up to 4 mM for C_{12}-sucrose and C_{12}-lactose (Fig. 7A–C). These large current inductions by carbachol in the presence of the esters were not statistically different from those of control tissue exposed to 10 μM carbachol, indicating that the mucosa retains its ion transport secretory functionality. For the C_{12}-sucrose and C_{12}-lactose esters, however, a partial decrease of ΔI_{sc} to around 30 μA cm^{-2} in the response to carbachol was recorded only at the high concentration of 8 mM of these esters (Fig. 7A, B), indicating some reduction in the stimulated inward current compared to carbachol alone at this ester concentration. Overall, these data indicate that the esters do not reduce tissue functionality except at very high 8 mM concentrations of C_{12}-sucrose and C_{12}-lactose, but not C_{12}-trehalose.

3.7. Effect of esters on histology of rat colonic tissue mounted in the Ussing chambers

Finally, we compared the effects of the esters on rat colonic mucosa tissue histology to see if the relatively innocuous patterns observed with direct and indirect measures of in vitro toxicity could be mirrored in pathology assessments. The histology of colonic mucosae was examined following exposure to the sugar esters for 120 min over a concentration range of 0.5–8 mM (Fig. 8). Tissue exposed to KH buffer showed a healthy intact epithelium (Fig. 8A). The esters had a concentration-dependent effect on tissue damage. The rank order of histological damage was C_{12}-sucrose > C_{12}-lactose > C_{12}-trehalose. Tissue exposed to C_{12}-sucrose at 0.5 mM showed an intact epithelium with some oedema (Fig. 8 Bi), while 1 mM C_{12}-sucrose induced cell sloughing on the apical side with cellular debris observed above the epithelium (Fig. 8 Bii). At 2 mM C_{12}-sucrose, oedema and the presence of goblet cells were more pronounced (Fig. 8 Biii). These two histology changes increased as the concentration of C_{12}-sucrose was further increased (Fig. 8 Biv). At 8 mM C_{12}-sucrose, the epithelium was no longer intact (Figure Bv). Tissue exposed to C_{12}-lactose also showed mild cell sloughing and the epithelium similarly remained intact until 8 mM (Figure Ci-v). Overall, compared to the other sugar esters, C_{12}-trehalose induced fewer changes in the colonic epithelial histology and the epithelium remained intact even at the highest concentration, 8 mM.

These data are consistent with the findings of the other assays, summarised in Table 2. A concentration of 8 mM was required for C_{12}-sucrose and C_{12}-lactose to damage the colonic epithelium. Yet even at
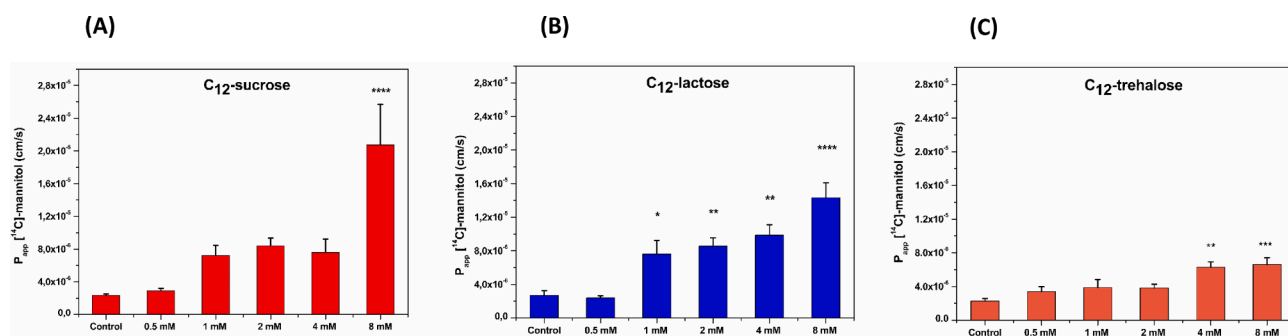
Fig. 6. Effect of (A) C_{12}-sucrose, (B) C_{12}-lactose, and (C) C_{12}-trehalose on the P_{app} of [^{14}C]-mannitol across rat colonic mucosae. Data are mean ± SEM (n = 4–8). Statistical significance was determined between respective treatments and control *P < 0.05; **P < 0.01; ***P < 0.001, ****P < 0.0001.
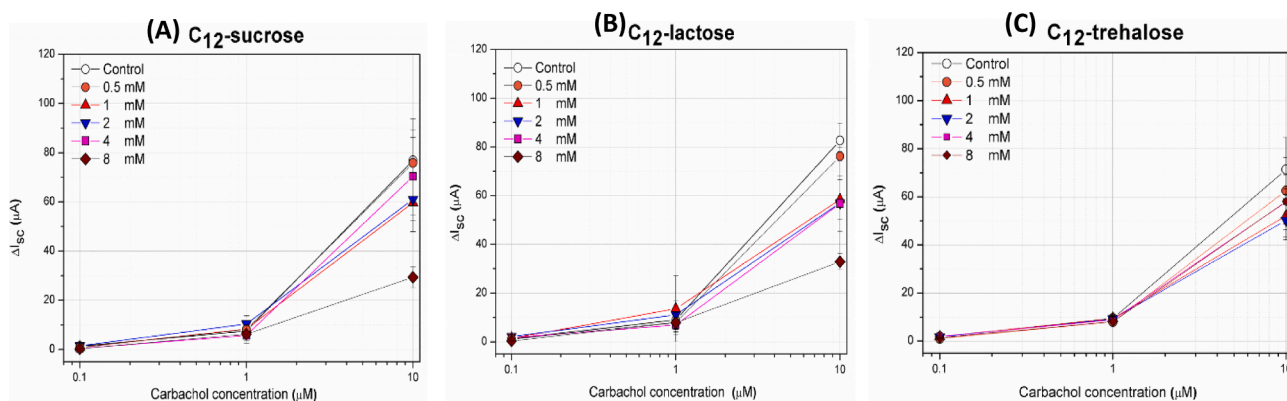
Fig. 7. Carbachol-induced Isc response of colonic mucosa after exposure to esters. (A) C_{12}-sucrose, (B) C_{12}-lactose, (C) C_{12}-trehalose. Data are mean $\pm$ SEM (n = 4–8).
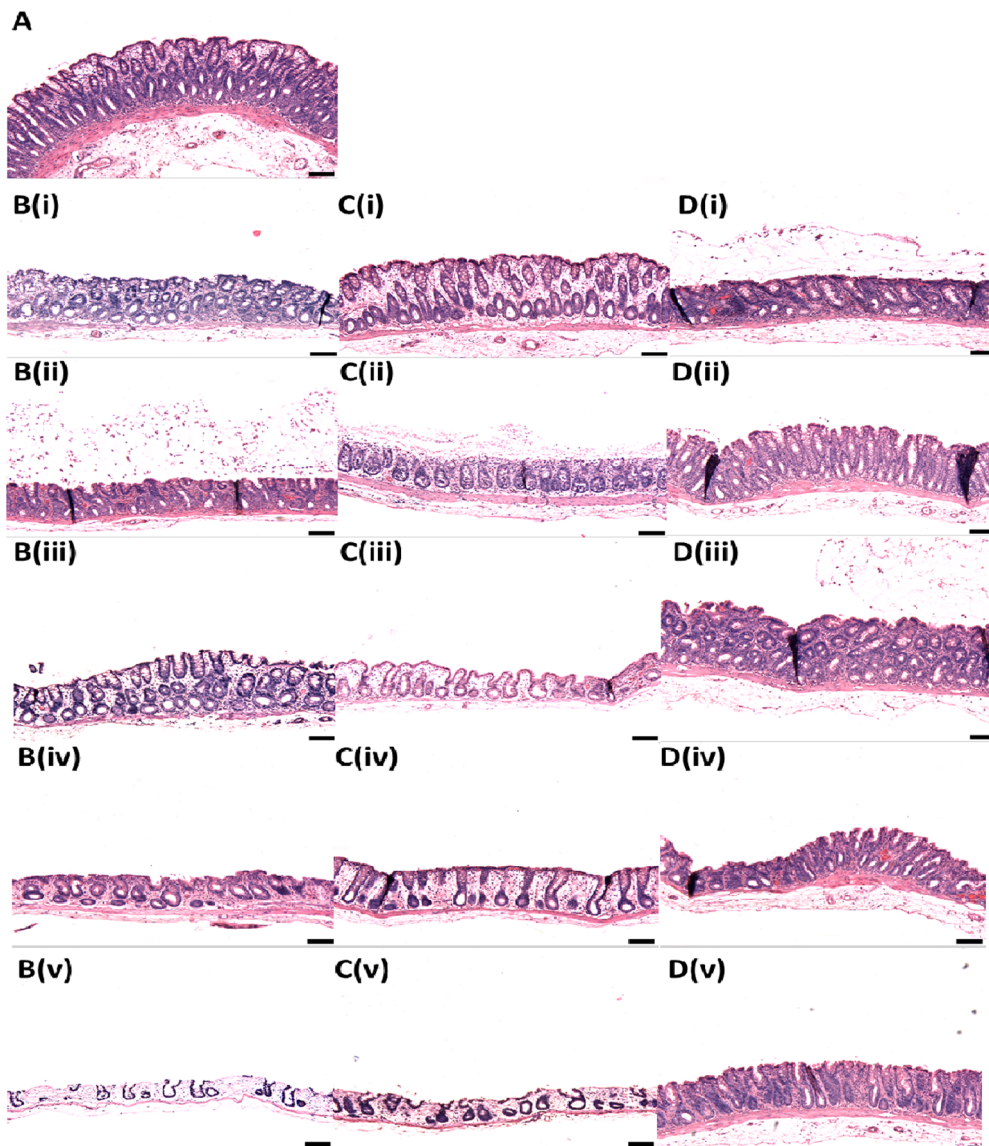

Fig. 8. Representative histology of rat colonic tissue mucosae stained with H & E after 120 min exposure to esters. (A) KH, (B) C_{12}-sucrose (C) C_{12}-lactose, (D) C_{12}-trehalose. Subscripts denote concentrations: (i) 0.5 mM, (ii) 1 mM (iii) 2 mM (iv) 4.0 mM (v) 8.0 mM. Scale bar = 100 μm.

this concentration, the tissue still retained the capacity to generate a stimulated I_{sc}, albeit somewhat reduced. Previous studies investigating sucrose laurate (D1216) and sodium caprate in the rat intestinal instillation *in vivo* model showed that at concentrations up to 25 mM no major effects were seen on colonic histology (McCartney et al., 2019a). This difference in sensitivity to PEs between the *ex vivo* and *in vivo*

Table 2
Summary of assay data for the monoester sugars.

	MTS TD$_{50}$ (mM)	LDHTD$_{50}$ (mM)	GP (1 mM)	TEER reduction	P$_{app}$ increase (4 mM)	Carbachol I$_{sc}$ loss (8 mM)	Tissue damage (8 mM)
C$_{12}$-sucrose	0.28	0.27	0.140	+++	3.6-fold	30–50%	+++
C$_{12}$-lactose	0.36	0.34	0.152	+++	3.7-fold	30–50%	++
C$_{12}$-trehalose	0.48	0.41	0.174	++	2.5-fold	10%	+

CMC data is in Table 1. MTS LDH and Laurdan GP (generalised polarisation) data was obtained in Caco-2 cells. TEER, P$_{app}$ of [^{14}C]-mannitol and histology data were obtained in isolated rat colonic mucosae. The Papp data was not significant for C$_{12}$-trehalose. TD$_{50}$: concentration that yields 50% cytotoxicity.

bioassays has been ascribed to several factors including the presence of a blood supply and capacity to repair and turn over epithelia in the instillation model (Maher et al., 2020). Compared to C$_{12}$-sucrose and C$_{12}$-lactose, C$_{12}$-trehalose was more benign concerning induction of tissue damage, consistent with its lower potency and efficacy on the [^{14}C]-mannitol P$_{app}$ and TEER reductions across colonic mucosae, as well as its higher TC$_{50}$ values in the MTT and LDH assays on Caco-2 cells.

4. Conclusions

This study has highlighted subtle differences in capacity for permeation enhancement between a set of disaccharides conjugated to the medium-fatty acid, C$_{12}$. We have expanded upon a previous discovery that a blend of food-derived sucrose laurate esters can act as intestinal PE and have shown that a fine chemical monoester form of it, designated as C$_{12}$-sucrose, can act similarly in an *ex vivo* model. By replacing sucrose with lactose or trehalose in the monoester, much of the same type of data was obtained. These non-ionic surfactants were relatively non-toxic on Caco-2 cells and acted primarily by fluidizing the apical membrane in these cells, typical of mild detergents. In the colonic tissue model, the mode of action arising from this initial event led to an opening of tight junctions and a resulting increase in paracellular flux at concentrations below those which caused membrane perturbation and tissue damage. On the other hand, the trehalose monoester was less potent and efficacious in all of the assays, likely arising from its lower CMC than the other two agents. Replacement of the disaccharide moiety in the laurate ester can cause subtle changes to the overall capacity as a PE.

The differences between the three esters across these assays raise questions about their mechanism of action as PEs on gut epithelia. A major PE, lauric acid (C$_{12}$), is likely to be liberated to some extent at the tissue by intestinal tissue esterases to exert its established effects as a membrane-fluidising surfactant (Brayden et al., 2014) and tight junction opener (Dittmann et al., 2014). However, since these esters do not quite have the same efficacy as PEs in the isolated rat intestinal mucosae, there is likely to be a contribution from the parent sugars where some differences are conferred by CMC values. This argument was also applied to previous studies of Labrasol® (comprising PEG esters and monoglycerides of C$_8$ and C$_{10}$) as a functional excipient, where it was argued that Labrasol® was behaving as a prodrug and that subsequent effects were down to lipase-liberated substrates (Fernandez et al., 2007). This conclusion was confounded in rat intestinal instillations studies *in vivo* when the PE effects were maintained for Labrasol® even in the presence of the lipase inhibitor (McCartney et al., 2019b).

Finally, we note that monoester formats of the three sugar-based surfactants can be made by simple green chemistry to yield pure products. This is relevant if these new PEs, some with efficacy on a par with medium-chain fatty acids, are eventually incorporated into oral dosage forms under Good Manufacturing Practice.

Funding

CRediT authorship contribution statement

Fiona McCartney: Conceptualization, Data curation, Formal analysis, Investigation, Methodology, Writing - review & editing. **Diego R. Perinelli:** Conceptualization, Investigation, Methodology, Writing - review & editing. **Mattia Tiboni:** Investigation, Methodology, Formal analysis. **Robert Cavanagh:** Methodology, Investigation, Formal analysis. **Simone Lucarini:** Investigation, Methodology, Formal analysis. **Giovanni Filippo Palmieri:** Investigation, Methodology, Formal analysis. **Luca Casettari:** Funding acquisition, Conceptualization, Investigation, Methodology, Project administration, Resources, Supervision, Writing - review & editing. **David J. Brayden:** Funding acquisition, Conceptualization, Methodology, Project administration, Resources, Supervision, Writing - original draft, Writing - review & editing.

Declaration of Competing Interest

The authors declare that they have no known competing financial interests or personal relationships that could have appeared to influence the work reported in this paper.

References

Antonescu, I.E., Rasmussen, K.F., Neuhoff, S., Fretté, X., Karlgren, M., Bergström, C.A.S., Nielsen, C.U., Steffansen, B., 2019. The permeation of acamprosate is predominantly caused by paracellular diffusion across Caco-2 cell monolayers: a paracellular modelling approach. Mol. Pharm. 16 (11), 4636–4650. https://doi.org/10.1021/acs.molpharmaceut.9b00733.

Baghban, A., Sasanipour, J., Sarafbidabad, M., Piri, A., Razavi, R., 2018. On the prediction of critical micelle concentration for sugar-based non-ionic surfactants. Chem. Phys. Lipids 214, 46–57. https://doi.org/10.1016/J.CHEMPHYSLIP.2018.05.008.

Brayden, D.J., Gleeson, J.G., Walsh, E.G., 2014. A head-to-head multi-parametric high content analysis of a series of medium-chain fatty acid intestinal permeation enhancers in Caco-2 cells. Eur. J. Pharm. Biopharm. 88 (3), 830–839.

Brayden, D.J., Hill, T.A., Fairlie, D.P., Maher, S., Mrsny, R.J., 2020. Systemic delivery of peptides by the oral route: formulation and medicinal chemistry approaches. Adv. Drug Deliv. Rev. 157, 2–36. https://doi.org/10.1016/J.ADDR.2020.05.007.

Bzik, V.A., Brayden, D.J., 2016. An assessment of the permeation enhancer, 1-phenyl-piperazine (PPZ), on paracellular flux across rat intestinal mucosae in Ussing chambers. Pharm. Res. 33 (10), 2506–2516. https://doi.org/10.1007/s11095-016-1975-4.

Buckley, S.T., Bækdal, T.A., Vegge, A., Maarbjerg, S.J., Pyke, C., Ahnfelt-Rønne, J., Madsen, K.G., Schéele, S.G., Alanentalo, T., Kirk, R.K., Pedersen, B.L., Skyggebjerg, R.B., Benie, A.J., Strauss, H.M., Wahlund, P.O., Bjerregaard, S., Farkas, E., Fekete, C., Søndergaard, F.L., Borregaard, J., Hartoft-Nielsen, M.L., Knudsen, L.B., 2018. Transcellular stomach absorption of a derivatized glucagon-like peptide-1 receptor agonist. Sci. Transl. Med. 10 (467) https://doi.org/10.1126/scitranslmed.aar7047 eaar7047.

Cavanagh, R.J., Smith, P.A., Stolnik, S., 2019. Exposure to a non-ionic surfactant induces a response akin to heat-shock apoptosis in intestinal epithelial cells: implications for excipient safety. Mol. Pharm. 16 (2), 618–631. https://doi.org/10.1021/acs.molpharmaceut.8b00934.

Dittmann, I., Amasheh, M., Krug, S.M., Markov, A.G., Fromm, M., Amasheh, S., 2014. Laurate permeabilizes the paracellular pathway for small molecules in the intestinal epithelial cell model HT-29, B6 via opening the tight junctions by reversible relocation of claudin-5. Pharm. Res. 31, 2539–2548. https://doi.org/10.1007/s11095-014-1350-2.

Elmowafy, E., El-Derany, M.O., Biondo, F., Tiboni, M., Casettari, L., Soliman, M.E., 2020. Quercetin loaded monolaurate sugar esters-based niosomes: sustained release and mutual antioxidant-hepatoprotective interplay. Pharmaceutics 12 (2), 143. https://doi.org/10.3390/pharmaceutics12020143.

Fernandez, S., Jannin, V., Rodier, J.D., Ritter, N., Mahler, B., Carrière, F., 2007. Comparative study on digestive lipase activities on the self emulsifying excipient Labrasol®, medium chain glycerides and PEG esters. Biochim. Biophys. Acta 1771 (5), 633–640. https://doi.org/10.1016/j.bbalip.2007.02.009.

Garofalakis, G., Murray, B.S., Sarney, D.B., 2000. Surface activity and critical aggregation concentration of pure sugar esters with different sugar headgroups. J. Colloid Interface Sci. 229, 391–398 https://doi.org/10.1006.

Gaudin, T., Rotureau, P., Pezron, I., Fayet, G., 2018. Investigating the impact of sugar-based surfactants structure on surface tension at critical micelle concentration with structure-property relationships. J. Colloid Interface Sci. 516, 162–171. https://doi.org/10.1016/J.JCIS.2018.01.051.

GraphPad Software, Segmental linear regression KNOWLEDGEBASE - ARTICLE #1101 https://www.graphpad.com/support/faq/segmental-linear-regression/ (accessed February 4, 2021).

Izutsu, K., 2018. Applications of freezing and freeze-drying in pharmaceutical formulations. iAdv. Exp. Med. Biol. 1081, 371–383. https://doi.org/10.1007/978-981-13-1244-1_20.

Kiss, L., Hellinger, É, Pilbat, A.M., Kittel, Á., Török, Z., Füredi, A., Szakács, G., Veszelka, S., Sipos, P., Ózsvári, B., Puskás, L.G., Vastag, M., Szabó-Révész, P., Deli, M.A., 2014. Sucrose esters increase drug penetration, but do not inhibit p-glycoprotein in Caco-2 intestinal epithelial cells. J. Pharm. Sci. 103 (10), 3107–3119. https://doi.org/10.1002/jps.24085.

Lichtenberg, D., Ahyayauch, H., Goñi, F.M., 2013. The mechanism of detergent solubilization of lipid bilayers. Biophys. J. 105 (2), 289–299. https://doi.org/10.1016/j.bpj.2013.06.007.

Lucarini, S., Fagioli, L., Campana, R., Cole, H., Duranti, A., Baffone, W., Vllasaliu, D., Casettari, L., 2016. Unsaturated fatty acids lactose esters: cytotoxicity, permeability enhancement and antimicrobial activity. Eur. J. Pharm. Biopharm. 107, 88–96. https://doi.org/10.1016/j.ejpb.2016.06.022.

Lucarini, S., Fagioli, L., Cavanagh, R., Liang, W., Perinelli, D.R., Campana, M., Stolnik, S., Lam, J.K.W., Casettari, L., Duranti, A., 2018. Synthesis, structure-activity relationships and in vitro toxicity profile of lactose-based fatty acid monoesters as possible drug permeability enhancers. Pharmaceutics 10 (3), 81. https://doi.org/10.3390/pharmaceutics10030081.

Maher, S., Kennelly, R., Bzik, V.A., Baird, A.W., Wang, X., Winter, D., Brayden, D.J., 2009. Evaluation of intestinal absorption enhancement and local mucosal toxicity of two promoters. I. Studies in isolated rat and human colonic mucosae. Eur. J. Pharm. Sci. 38 (4), 291–300. https://doi.org/10.1016/j.ejps.2009.09.001.

Maher, S., Heade, J., McCartney, F., Waters, S., Bleiel, S.B., Brayden, D.J., 2018. Effects of surfactant-based permeation enhancers on mannitol permeability, histology, and electrogenic ion transport responses in excised rat colonic mucosae. Int. J. Pharm. 539 (1–2), 11–22. https://doi.org/10.1016/j.ijpharm.2018.01.008.

Maher, S., Geoghegan, C., Brayden, D.J. 2020. Intestinal permeation enhancers to improve oral bioavailability of macromolecules: reasons for low efficacy in humans. Expert. Opin. Drug. Deliv. Sep 29:1–28. doi: http://dx.doi.org/10.1080/17425247.2021.1825375.

Mine, Y., Zhang, J.W., 2003. Surfactants enhance the tight-junction permeability of food allergens in human intestinal epithelial Caco-2 cells. Int. Arch. Allergy Immunol. 130 (2), 135–142. https://doi.org/10.1159/000069009.

McCartney, F. Rosa, M. Brayden, D.J. 2019a. Evaluation of sucrose laurate as an intestinal permeation enhancer for macromolecules: ex vivo and in vivo studies. Pharmaceutics. 11 (11) 565. https://doi.org/10.3390/pharmaceutics11110565.

McCartney, F., Jannin, V., Chevrier, S., Boulghobra, H., Hristov, D.R., Ritter, N., Miolane, C., Chavant, Y., Demarne, F., Brayden, D.J., 2019b. Labrasol® is an efficacious intestinal permeation enhancer across rat intestine: ex vivo and in vivo rat studies. J. Control. Release. 310, 115–126.

Parasassi, T., De Stasio, G., Ravagnan, G., Rusch, R.M., Gratton, E., 1991. Quantitation of lipid phases in phospholipid vesicles by the generalized polarization of Laurdan fluorescence. Biophys. J. 60 (1), 179–189. https://doi.org/10.1016/S0006-3495(91)82041-0.

Preté, Paulo S.C., Domingues, Cleyton C., Meirelles, Nilce C., Malheiros, Sônia V.P., Goñi, Félix M., de Paula, Eneida, Schreier, Shirley, 2011. Multiple stages of detergent-erythrocyte membrane interaction-A spin-label study. Biochim. Biophys. Acta – Biomembr. 1808 (1), 164–170. https://doi.org/10.1016/j.bbamem.2010.10.016.

Sanchez, S.A., Tricerri, M.A.E., Gratton, E., 2012. Laurdan generalized polarization fluctuations measures membrane packing micro-heterogeneity in vivo. PNAS USA 109, 7314–7319.

Shubber, S., Vllasaliu, D., Rauch, C., Jordan, F., Illum, L., Stolnik, S., Mechanism of mucosal permeability enhancement of CriticalSorb® (Solutol® HS15) investigated in vitro in cell cultures. 2015. Pharm. Res. 32, 516–527. https://doi.org/10.1007/s11095-014-1481-5.

Stuettgen, V., Brayden, D.J., 2020. Investigations of piperazine derivatives as intestinal permeation enhancers in isolated rat intestinal tissue mucosae. AAPS J. 22 (2), 33. https://doi.org/10.1208/s12248-020-0416-9.

Tuvia, S., Atsmon, J., Teichman, S.L., Katz, S., Salama, P., Pelled, D., Landau, I., Karmeli, I., Bidlingmaier, M., Strasburger, C.J., Kleinberg, D.L., Melmed, S., Mamluk, R., 2012. Oral octreotide absorption in human subjects: comparable pharmacokinetics to parenteral octreotide and effective growth hormone suppression. J. Clin. Endocrinol. Metab. 97 (7), 2362–2369. https://doi.org/10.1210/jc.2012-1179.

Twarog, C., McCartney, F., Harrison, S.M., Illel, B., Fattal, E., Brayden, D.J., 2021. Comparison of the effects of the intestinal permeation enhancers, SNAC and sodium caprate (C_{10}): isolated rat intestinal mucosae and sacs. Eur. J. Pharm. Sci. 158, 105685. https://doi.org/10.1016/j.ejps.2020.105685.

Verstraeten, S.V., Jaggers, G.K., Fraga, C.G., Oteiza, P.I., 2013. Procyanidins can interact with Caco-2 cell membrane lipid rafts: involvement of cholesterolProcyanidins can interact with Caco-2 cell membrane lipid rafts: Involvement of cholesterol. Biochim. Biophys. Acta - Biomembr. 1828 (11), 2646–2653. https://doi.org/10.1016/j.bbamem.2013.07.023.

von Erlach, T., Saxton, S., Shi, Y., Minahan, D., Reker, D., Javid, F., Lee, Y.-Ah L., Schoellhammer, C., Esfandiary, T., Cleveland, C., Booth, L., Lin, J., Levy, H., Blackburn, S., Hayward, A., Langer, R., Traverso, G., 2020. Robotically handled whole-tissue culture system for the screening of oral drug formulations. Nat. Biomed. Eng. 4 (5), 544–559. https://doi.org/10.1038/s41551-020-0545-6.